ridges or grooves [figure 24C in (5)]. This unit is a subdivision of larger, more complex geomorphologic regions called tesserae (23, 26) and has formed by complex deformation (5). (ii) Ridged terrain occurs at high elevations (>1 km above mean planetary radius) and is characterized by long (>100 km) ridges and valleys that are commonly cut by shorter grooves and ridges. Both linear and equidimensional ridged terrains are seen (Fig. 3). The mountains are interpreted to have formed from compressional deformation, followed in some areas by extension (5). Two types of linear belts, typically 30 to 50 km wide (23), have been identified on the basis of the dominant tectonic feature. (iii) Ridge belts, a large group of which are found in Lavinia Planitia [figure 6 in (5)] are commonly cut by grooves. Ridges tend to lie in belts of high radar cross section that is attributed to increased roughness resulting from tectonic disruption. Ridge belts tend to extend for hundreds of kilometers and to have relief of 1 km or less. They are interpreted to be compressional in origin; some are cut by later episodes of extensional deformation (5). (iv) Groove belts are belts of linear structures dominated by grooves typically spaced 5 to 20 km apart [figure 37C in (5)]. The belts are associated with areas of raised topographic relief, typically higher than in ridge belts. The grooves are interpreted to be local extensional features over areas of compression (5).

Magellan data have revealed a number of surficial material units not previously identified, with the exception of crater materials: (i) Crater materials are deposits located within and surrounding craters and are characterized by high radar cross sections [figure 1A in (7)]. Material surrounding craters generally has lobate boundaries and a hummocky appearance, and is interpreted to be of impact origin (7). (ii) Channel materials are generally sinuous with a low radar backscatter cross section. Channels are 1 to 3 km across, are located in plains and highland regions [figure 17A in (6)], and are interpreted to be lava channels or sinuous rilles (6). (iii) Bright lobate surficial materials have variable radar cross section and are contiguous with crater materials. They extend from 50 to 200 km; their emplacement tends to be topographically controlled (Fig. 4). These units are interpreted to result from outflow of highly fluid material, probably volcanic in origin, caused by the cratering process (7). (iv) Bright material (high radar cross section) appears to be contiguous with ridges or small domical hills in many areas or appears as long (>100 km) linear units. Some bright areas have a feathered appearance [figure 8 in (4)] and are interpreted to be regions of increased surface roughness created by deposition or removal of material by wind. (v) Many regions contain circular or elongate, dark diffuse materials [figures 8 in (4) and 6C in (7)]. Dark material is interpreted to be areas of increased smoothness due to deposition of fine material. (vi) Linear faceted material occurs in groups of lineations, typically extending for <100 km [figure 8 in (4)]. This unit may represent sand dunes (4).

Initial analysis of Magellan data has revealed the complex nature of volcanic and tectonic processes that have affected the planet's surface. Unexpected initial results include the great variety of volcanic landforms, the intensity of tectonic processes, and the outflow features associated with impact craters. Further analysis and mapping to obtain a global understanding of the geologic history of Venus, and detailed comparisons with geologic processes on other planets (including Earth) are ongoing.

REFERENCES AND NOTES

1. S. C. Solomon and J. W. Head, *Science* **252**, 252 (1991).
2. R. S. Saunders and G. H. Pettengill, *ibid.*, p. **247**.
3. G. H. Pettengill, P. G. Ford, W. K. Johnson, R. K. Raney, L. A. Soderblom, *ibid.*, p. **260**.
4. R. Arvidson, V. Baker, C. Elachi, R. S. Saunders, J. Wood, *ibid.*, p. **270**.
5. S. C. Solomon *et al.*, *ibid.*, p. 297.
6. J. W. Head *et al.*, *ibid.*, p. 276.
7. R. J. Phillips *et al.*, *ibid.*, p. 288.
8. C. P. Florensky *et al.*, *Geol. Soc. Am. Bull.* **88**, 1537 (1977).
9. A. T. Basilevsky *et al.*, *ibid.* **96**, 137 (1985).
10. A. T. Basilevsky and Yu. A. Surkov, *V-Gram* (no. 1) (Jet Propulsion Laboratory, Pasadena, CA, 1989); *ibid.*, no. 2.
11. O. V. Nikolayeva, *Earth Moon Planets* **50–51**, 329 (1990).
12. C. M. Pieters *et al.*, *Science* **234**, 1379 (1986).
13. A. S. Selivanov *et al.*, *Kosm. Issled.* **21** (no. 2), 176 (1983).
14. R. M. Goldstein *et al.*, *J. Geophys. Res.* **81**, 4807 (1976); *Icarus* **36**, 334 (1978); D. B. Campbell and B. A. Burns, *J. Geophys. Res.* **85**, 8271 (1980); D. B. Campbell *et al.*, *Science* **246**, 373 (1989).
15. G. E. McGill, S. J. Steenstrup, C. Barton, P. G. Ford, *Geophys. Res. Lett.* **8**, 737 (1981); D. B. Campbell *et al.*, *Science* **226**, 167 (1984); E. R. Stofan *et al.*, *Geol. Soc. Am. Bull.* **101**, 143 (1989).
16. D. B. Campbell, J. W. Head, J. K. Harmon, A. A. Hine, *Science* **221**, 644 (1983); L. C. Crumpler, J. W. Head, D. B. Campbell, *Geology* **14**, 1031 (1986).
17. D. B. Campbell, D. A. Senske, J. W. Head, A. A. Hine, P. C. Fisher, *Science* **251**, **180** (1991).
18. R. E. Arvidson, J. J. Plaut, R. F. Jurgens, R. S. Saunders, M. A. Slade, *Lunar Planet. Sci.* **20**, 25 (1989).
19. E. R. Stofan and R. S. Saunders, *Geophys. Res. Lett.* **17**, 1377 (1990).
20. H. Masursky *et al.*, *J. Geophys. Res.* **85**, 8232 (1980).
21. G. H. Pettengill et al., *ibid.*, p. 8261.
22. W. L. Sjogren *et al.*, *ibid.* **88**, 1119 (1983).
23. V. L. Barsukov *et al.*, *Proc. Lunar Planet. Sci. Conf.* **16**, *J. Geophys. Res.* **91**, B4, D378 (1986); A. T. Basilevsky *et al.*, *ibid.*, p. D399.
24. B. A. Ivanov *et al.*, *ibid.*, p. D413; A. T. Basilevsky and J. W. Head, *Annu. Rev. Earth Planet. Sci.* **16**, 295 (1988); G. G. Schaber, *U.S. Geol. Surv. Open-File Rep. 90-468* (1990), p. 57.
25. R. E. Arvidson, R. E. Grimm, R. J. Phillips, G. G. Schaber, E. M. Shoemaker, *Geophys. Res. Lett.* **17**, 1385 (1990).
26. A. L. Sukhanov *et al.*, *U.S. Geol. Surv. Map 1-2059, V15M90/0G* (1989); V. A. Kotelnikov *et al.*, *Atlas Poverkhnosti Venery* (Atlas of Venus Surface) (Moscow Gugk, 1989); G. G. Schaber and R. C. Kozak, *U.S. Geol. Surv. Open-File Map 90-24*, 1:15,000,000 scale (1990).
27. G. L. Tyler *et al.*, *Science* **252**, 265 (1991).

28. This work was conducted at the Jet Propulsion Laboratory, California Institute of Technology, under contract with the National Aeronautics and Space Administration. This work was supported in part by various Magellan contracts from the Jet Propulsion Laboratory to the authors' home institutions. E.R.S. was supported by a National Academy of Sciences—National Research Council Associateship. We would like to thank A. T. Basilevsky, E. deJong, D. Senske, T. Parker, C. Leff, M. Jasnow, and S. Yewell for their contributions.

25 January 1991; accepted 22 March 1991

Fundamental Issues in the Geology and Geophysics of Venus

SEAN C. SOLOMON AND JAMES W. HEAD

A number of important and currently unresolved issues in the global geology and geophysics of Venus will be addressable with the radar imaging, altimetry, and gravity measurements now forthcoming from the Magellan mission. Among these are the global volcanic flux and the rate of formation of new crust; the global heat flux and its regional variations; the relative importance of localized hot spots and linear centers of crustal spreading to crustal formation and tectonics; and the planform of mantle convection on Venus and the nature of the interactions among interior convective flow, near-surface deformation, and magmatism.

ONE OF THREE DISTINCT MECHANISMS dominates global heat transport across the lithosphere (1) of solid planets and satellites: (i) recycling of lithospheric plates (as on Earth), (ii) hotspot volcanism (as on Io), or (iii) simple conduction through a globally continuous lithospheric shell (as on the smaller terrestrial planets). The mechanism of lithospheric heat transport on a planet is fundamentally linked to its tectonic and volcanic evolution. The dominant lithospheric heat transport mechanism on Venus—the planet most sim-

S. C. Solomon, Department of Earth, Atmospheric, and Planetary Sciences, Massachusetts Institute of Technology, Cambridge, MA 02139.
J. W. Head, Department of Geological Sciences, Brown University, Providence, RI 02912.

ilar to Earth in terms of mass, radius, and bulk composition—has been a matter for debate since the Pioneer Venus mission (*2, 3*), but results from the subsequent Venera and Vega missions and from Earth-based radar imaging have restricted the potential contributions from the first two mechanisms. Less well understood are the processes by which chemically distinct crust formed on Venus, the characteristics and planform of its mantle convection, and the nature of the interaction of mantle convective flow with the overlying lithosphere. In order to place the new information received from the Magellan spacecraft in context with respect to these questions, we synthesize what is known about the geophysical workings of Venus, highlight the most important unresolved issues, and discuss how Magellan data may help to resolve these issues.

Global geological processes and tectonic patterns. Exploration of Venus by the United States and the Soviet Union before the Magellan mission has provided sufficient data to characterize the nature and distribution of regional geological structures and deposits over approximately 45% of the surface imaged at a resolution of 1 to 4 km and has revealed the long-wavelength topography over about 90% of the surface. Elevations on Venus have a unimodal distribution (*4*) in contrast to the bimodal distribution of elevations on Earth; 80% of Venus' surface consists of plains at elevations within 1 km of the modal value (*5*). The dominant topographic features are the equatorial highlands, flanking mid-latitude lows, and high-latitude uplands (Fig. 1A). Venus also displays prominent long-wavelength variations in gravity (Fig. 1B) that, in striking contrast to those on Earth, are strongly correlated with long-wavelength topography (*2, 6*).

The density of impact craters and basins on Venus is considerably less than on the smaller terrestrial planets, the moon, Mars, and Mercury, which have surfaces formed largely in the first half of solar system history. On the 45% of the surface of Venus seen by Earth-based and orbital radar, the density of craters interpreted to be of impact origin and greater than about 8 km in diameter is about 1 per 10^6 km^2. The size-frequency distribution of these craters is generally interpreted to represent an age of less than about 10^9 years (*7*). No large multi-ringed impact basins with diameters in excess of

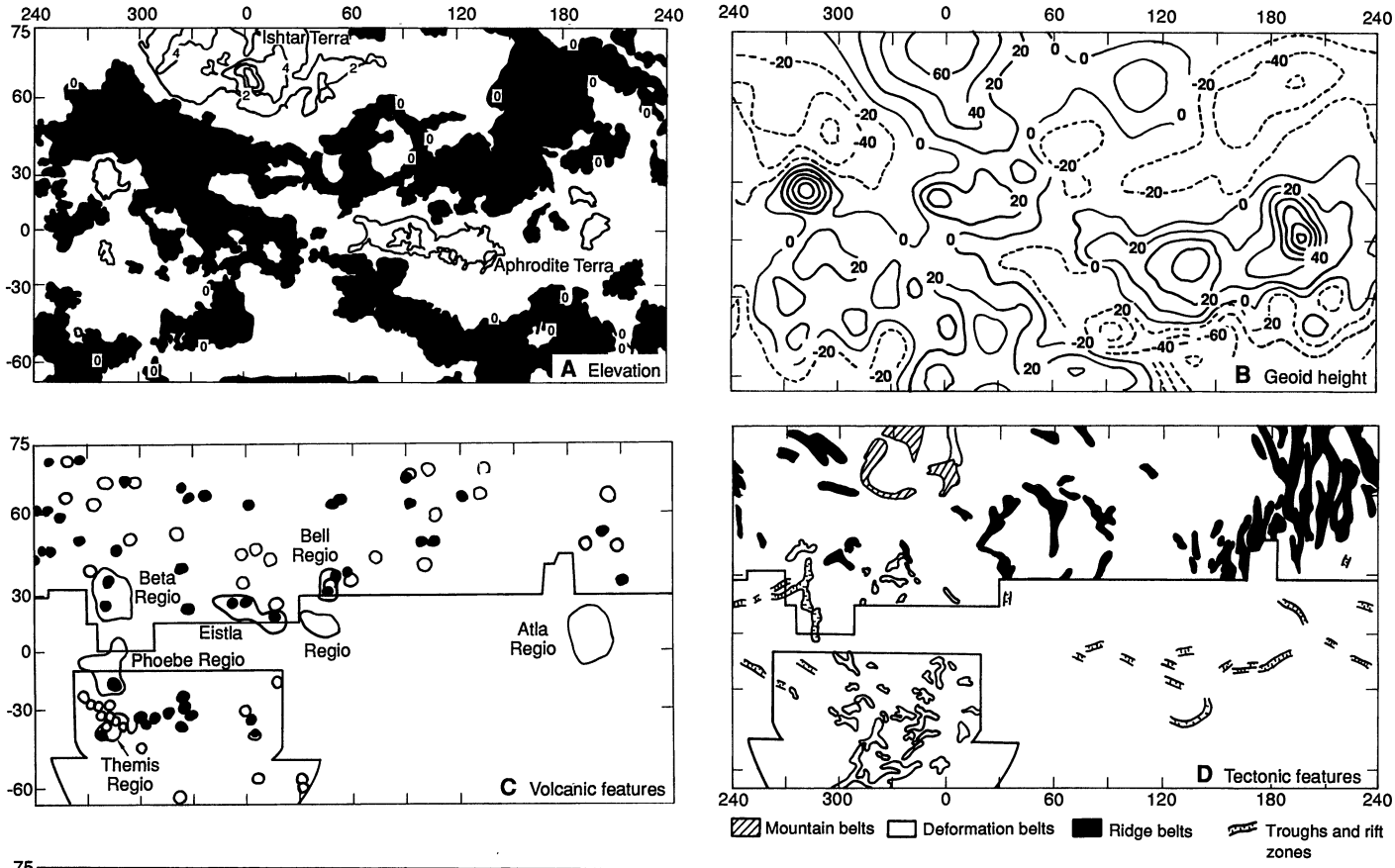

Fig. 1. Simplified maps of geological and geophysical features of Venus. (**A**) Global topography (*4*). Datum is a sphere of radius 6051.9 km; 2-km contour interval. Areas below datum are in black. (**B**) Global geoid (*6*). Twenty-meter contour interval; negative contours are dashed. (**C**) Major volcanic features identified from Venera 15–16 and Arecibo images (areas of coverage are delimited by solid lines). Volcanic edifices exceeding 100 km in basal diameter (*11, 14, 19, 33*) are shown as solid circles. Coronae in excess of 200 km in diameter (*11, 17, 18, 33*) are shown as open circles. Broad rises 2000 to 3000 km in extent are indicated by name. (**D**) Major tectonic features. Mountain belts surrounding Lakshmi Planum are indicated by ruling. Ridge belts identified in Venera 15–16 data are shown in black, and deformation belts identified from Arecibo images are outlined (*11, 32, 33*). The resolution and viewing geometry of Arecibo images do not permit distinguishing between ridge belts and groove belts for most southern hemisphere features shown. (**E**) Areas of tessera terrain identified in Venera 15–16 and Arecibo images (*11, 33*) are shown in black.

160 km have been identified from Venera or Arecibo images, consistent with such an age. The average age of the surface of Venus appears, on this basis, to be much younger than those of the smaller terrestrial planetary bodies but somewhat older than that of Earth (*8*).

The formation of sediment and its erosion, transport, and redeposition are thought to be much less important on Venus than on Earth or even the other terrestrial planets. The dense Venus atmosphere prevents small meteoroids from impacting the surface; the impact of such objects on the moon has fragmented surface material and led to global regolith formation. The lack of water and thermal cycling on Venus severely limits chemical and physical weathering and subsequent transport of surface materials. Geological processes such as the formation of large impact craters, tectonic activity, and possibly pyroclastic volcanism can provide local sources of sediment, and eolian activity is capable of sediment transport (*9*), but the fraction of the surface that contains significant thicknesses of soil deposits appears to be small (*10*). Whether Venus preserves a record of an early climate in which atmospheric mass or surface temperature were significantly different from the present is an important question that data from Magellan should answer.

Volcanism has been widespread on Venus; volcanic deposits form more than 70% of the surface units mapped in the areas well imaged before the Magellan mission. Regional plains units interpreted to be of volcanic origin (*11*) on the basis of their regional topography and smoothness, associated flows, and nearly ubiquitous small shields (*12*) are the most abundant unit. Localized centers of volcanism have produced edifices spanning a large range in sizes (Fig. 1C). About 800 volcanoes between 20 and 100 km in diameter have been mapped in the 25% of the surface imaged by Venera 15 and 16 (*13*), and approximately 50 shield volcanoes, large calderas, and distinctive volcanic centers greater than 100 km in diameter have been mapped from Venera and Arecibo images covering about 45% of the surface (*11, 14*). No data are available, however, on the relative or absolute ages of these structures. Coronae (Fig. 1C), circular to oval structures 200 to 1000 km in diameter with a generally elevated center and a narrow deformed annulus of concentric ridges (*15*), have been interpreted as products of local plume-like mantle upwelling on the basis of their general characteristics, their approximately circular symmetry, and the presence of volcanic sources and deposits in their interiors (*16, 17*). Many coronae are clustered, as around Themis Regio and east and west of Ishtar Terra (Fig. 1C). Approximately 20 to 30 coronae have been mapped in the area of Venera 15–16 imaging (*17*), and although there may be an age sequence on the basis of morphology and apparent stage of development (*18*), specific ages and the distribution of those coronae recently or even currently active has not been determined. Volcanism is also concentrated in broad topographic rises 1000 to 3000 km in diameter (Fig. 1C), predominantly in and near the equatorial highlands (*11, 19–21*). These structures vary in topographic form from broad rises (Beta, Bell, and Atla Regiones) to plateau-like features (Ovda and Thetis Regiones). On the basis of their large apparent depths of compensation of long-wavelength relief (*22*) and detailed radar images of selected areas (*19, 23*), these rises are thought to be sites of mantle upwelling and associated volcanism at a larger scale than at coronae, but their detailed mode of formation and the relative contributions to topographic relief from thermal uplift, volcanism, and igneous intrusion are not known. In general, volcanism is widespread and is probably linked to mantle upwelling of a variety of different scales and geometries, but its role in the overall formation and evolution of the crust is not well understood.

A variety of features interpreted to be of tectonic origin are known on Venus. Rift zones 100 to 300 km wide, thousands of kilometers long, and up to 5 km in relief occur in many highland regions (*21, 24, 25*). The largest rifts are in the equatorial highlands and Beta-Phoebe Regiones (Fig. 1D); two prominent tectonic junctions occur at Beta and Atla Regiones (*24*). The rift systems in Beta Regio have been interpreted as sites of only limited extension (tens of kilometers or less) and may be analogous to intracontinental rift zones on Earth (*25*). The rift systems along the 17,000-km-long portion of the equatorial highlands in Aphrodite Terra, in contrast, have been interpreted by some workers as marking a crustal spreading center analogous to terrestrial mid-ocean ridges (*26, 27*). Evidence cited in favor of crustal spreading at Aphrodite includes bilateral symmetry in topography about the axis of highland segments and the presence of regional cross-strike discontinuities in topography and radar reflectivity oriented approximately orthogonal to the rise axis and showing some similarities to oceanic fracture zones (*28*).

In contrast to these extensional features, linear mountain belts in western Ishtar Terra that have local relief of 3 to 6 km and a cumulative length of about 4000 km have been inferred to be sites of orogeny (*29*) and associated underthrusting and shortening and thickening of the crust (*30, 31*). Outstanding questions include the mechanism and magnitude of the implied horizontal motions, the extent of recycling of crust into the mantle during episodes of active convergence, the evolution of orogenic belts once convergence and underthrusting cease, and the nature and distribution of regions that were products of mountain building earlier in geological history. Smaller but possibly analogous features in plains regions are the ridge belts, linear deformational features up to several hundred kilometers wide and hundreds to thousands of kilometers in length. Ridge belts form in two distinctive patterns: parallel to subparallel networks and fans within lowlands (Lavinia and Atalanta Planitiae areas) and more nearly orthogonal patterns adjacent or parallel to tessera blocks (Fig. 1D) (*32, 33*). These features are characterized by narrow ridges and arches and generally rise up to several hundred meters above the surrounding plains. The cumulative length of ridge belts mapped in the northern 25% of the planet is about 40,000 km (*32*). Their similarity to mare ridges and arches on the moon, their topographic forms, and their spacing (*34*) have led many authors to conclude that most formed predominantly by crustal shortening (*15, 16, 32, 35*). In an alternative view (*36*), ridge belts have been interpreted to be of extensional origin on the basis of the parallel pattern of ridges within them, their occasional occurrence in topographic lows, evidence for split and separated features, and their fan-like nature in Atalanta Planitia suggestive of crustal spreading. Imaging and topographic data from Magellan should permit the determination of the sense and perhaps the magnitude of strain across ridge belts, the distribution of such regions of concentrated strain, and their relation to global tectonic patterns.

In addition to the linear deformational zones dominated by both extension (such as rifts) and compression (such as mountain belts), there are more equidimensional regions of intense deformation (*16*) known as tesserae, which occupy about 10 to 15% of the area imaged by Venera 15 and 16 (Fig. 1E). Tesserae commonly are more elevated than adjacent plains and are characterized by at least two intersecting families of linear to arcuate deformational features. The patterns can be relatively simple and orthogonal, similar to patterns on the Earth's sea floor (*37*), or they can be much more varied and complex (*38*). A number of formational and modificational processes have been proposed to account for the elevated topography and deformational patterns of tesserae (*38*) including crustal divergence at a linear rise or local hot spot, convergence and crustal thickening, gravitational relaxation, and gravity sliding. On the basis of their diver-

sity and complexity, it is likely that tesserae result from a variety of processes. Data from Magellan will provide information on the style of deformation within individual tesserae, the relation between deformation and topographic slope, the spectrum of gravity signatures, and whether individual tessera terrains represent stages in a developmental sequence.

Interior heat budget. The heat budget of Venus' interior governs the planetary thermal history, the dynamics of the mantle, and the mechanical properties of the lithosphere. Cosmochemical considerations (*39*) and surface measurements of U, Th, and K (*40, 41*) suggest that radiogenic heat production in Venus is broadly similar to that in Earth. The atmospheric abundance of ^{40}Ar per planet mass is about one fourth to one third that of Earth (*42, 43*). This lower amount can be attributed to differences in the extent or timing of outgassing or in the bulk K abundance. The nearly terrestrial values for the K/U ratio in the crust (*40, 41*), however, support the inference that differences in outgassing have dominated (*43*), along with some contribution from a lesser degree of fractionation of K into the crust and a significantly lower rate of crustal erosion than on Earth.

If Venus loses heat at the same rate per mass as Earth, the mean heat flux would be about 70 mW m^{-2} (*3*); the uncertainty is perhaps 30% from possible differences in the K abundance and in the fraction of heat loss contributed by secular cooling of the planet (*39*) and by possible nonmonotonic variations in terrestrial heat loss (*44*). This heat flux, if derived mostly from beneath the crust, is sufficient to fuel vigorous mantle convection and is equivalent to an average conductive thermal gradient in the lithosphere of 15 to 30 K km^{-1}, depending on the crustal thickness and thermal conductivity structure. On Earth the fractional heat loss contributed by interior cooling may be as high as 50% (*45*). That fraction may be smaller for Venus if its interior has cooled more than that of Earth, perhaps because of more efficient mantle convection induced by the lower viscosity of its hotter lithosphere (*46*) or simply because it is a slightly smaller planet and thus has less thermal inertia (*47*). If so, then the average heat flux and lithospheric thermal gradients could be less than the above values. We return to this question below.

Although the prospects for direct measurement of surface heat flow on Venus are remote, the thermal gradient may be inferred indirectly from the thickness of the elastic lithosphere estimated from the flexural response to lithospheric loads (*48*). Before the Magellan mission, topography provided the only resolvable signature of flexure, and other contributors to topographic relief may mimic flexure (*49*). The most likely case of flexure yet identified is where the lithosphere of the North Polar Plains is interpreted as having underthrust Freyja Montes to the south (*31*); the flexural length scale indicates that the elastic lithosphere is 11 to 18 km thick, consistent with a thermal gradient of 15 to 25 K km^{-1} and a heat flow of 50 to 70 mW m^{-2} (*50*). Because the North Polar Plains stand at an elevation near the modal value for the planet, this range in heat flow is broadly consistent with the expectation that scaling global heat loss from Earth is a reasonable assumption and that regions on Venus at an elevation near the modal value have heat flow near the global average. The Magellan mission, through altimetry and high-resolution images of flexurally induced tectonic features in regions near lithospheric loads, should permit the estimation of elastic lithosphere thickness more widely on the planet.

Lithospheric heat transport mechanisms. Among the lithospheric heat transport mechanisms known to predominate on other planets and satellites, hot spot volcanism—also known as the heat pipe model (*51*)—is the most straightforward to quantify and to assess. If most of the heat were carried by magma rising rapidly from the asthenosphere to near-surface regions, then the conductive gradient throughout most of the lithosphere could be small and the crust and lithosphere could be thick, a situation that would permit support of the strongly correlated long-wavelength topography and gravity (*2, 6*) by some combination of Airy isostasy and lithospheric strength (*51*). Volcanic heat transport on Venus can account for the global heat loss, however, only if the volumetric flux of magma to the surface is about 200 km^3 yr^{-1} (*3, 51*). Two separate lines of argument have been advanced to suggest that the actual volcanic flux is lower than this value by at least two orders of magnitude. First, the surface density of impact craters imaged by Venera 15 and 16 (*52*), the probable upper limit on the crater production rate on Venus, and the assumption that impact cratering and volcanic resurfacing occur with equal probability over the entire surface yield an upper bound on the average volcanic flux of 2 km^3 yr^{-1} (*53*). This bound is lowered by up to an order of magnitude if many of the circular features of uncertain origin within the area of Venera 15–16 coverage (*52*) are actually degraded or modified impact structures (*54*). These figures would not constitute bounds if volcanic resurfacing were concentrated in localized areas controlled, say, by elevation or by mantle dynamic and thermal structure and if islands of older and more cratered terrain remained. Such a distribution does not appear to be the case for the part of Venus imaged by Venera 15 and 16 (*52*), but this question merits careful scrutiny with Magellan data. The second argument limiting volcanic flux (*55*) is based on the premise that volcanic replenishment of atmospheric SO_2 is necessary to maintain the global H_2SO_4 clouds. From measured rates of reaction between SO_2 and calcite ($CaCO_3$) to form anhydrite ($CaSO_4$), the required rate of volcanism is about 1 km^3 yr^{-1}; this rate has an uncertainty of at least an order of magnitude because of uncertainties in the average S abundance of Venusian magmas and in the dominant crustal sink for SO_2 (*55*). This line of reasoning has been challenged (*56*), however, on the grounds that calcite is not in equilibrium with the Venus atmosphere at any surface elevation and that the atmospheric SO_2 content is likely buffered by a reaction in which anhydrite is replaced by the pyroxene $CaMg(SiO_3)_2$. Regardless of whether the S cycle on Venus provides a useful constraint on volcanic flux, extrusive magmatism at a rate of 2 km^3 yr^{-1} or less contributes negligibly (~1% or less) to global heat loss (Fig. 2).

The role of plate recycling in the tectonic evolution of Venus remains open, but the contribution of creation and destruction of lithosphere to the present global heat loss

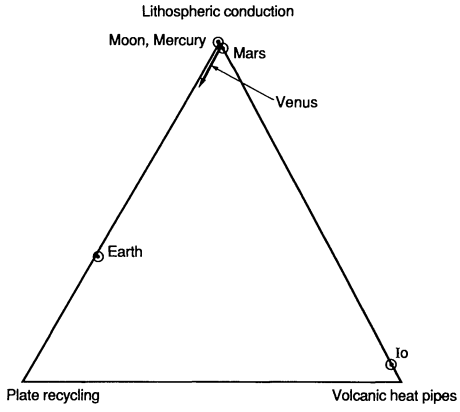

Fig. 2. Schematic ternary diagram showing the relative contributions of lithospheric heat transport mechanisms toward global heat loss on solid planets and satellites [after (*3*)]. Heat loss on Earth occurs mostly along the mid-ocean ridges by the processes of formation and cooling of oceanic lithosphere. Hot spot volcanism, or volcanic heat pipes (*51*), contributes negligibly to global heat loss on the moon, Mercury, Mars, and Earth and constitutes a significant heat transport mechanism only on Jupiter's moon Io. The range of possible positions for Venus permitted by impact crater density (*52*) and topographic constraints on lithospheric recycling rates (*26*) is indicated. Although lithospheric conduction appears to dominate heat loss on Venus, the heat flow is likely to be anomalously high over regions of mantle upwelling.

can, with a few simplifying assumptions, be bounded. As noted above, the equatorial highlands, marked by elevated topography, large free-air gravity anomalies, and numerous large-scale extensional and volcanic structures (*2, 5, 24*), are thought to be regions of crustal divergence. Whether they are more nearly analogous to continental rifts as proposed for Beta Regio (*25*), oceanic spreading centers as suggested for western Aphrodite Terra (*27*), or a collection of individual hot spots as proposed for all of the equatorial highlands (*57, 58*), however, has not been clear, largely because the key highland region, Aphrodite Terra, is wholly outside the areas that have been well imaged by Venera 15 and 16 and Earth-based radar. Imaging of Aphrodite Terra and other equatorial highlands by Magellan should provide key data to distinguish clearly among alternative interpretations.

Under the assumption that the equatorial highlands are analogues to oceanic spreading centers, local spreading rates inferred from the fall-off of topography with distance from the spreading axis are a few tens of millimeters per year (*26, 59*). For a total length of spreading center segments of 2×10^4 km the areal rate of creation of new lithosphere has been estimated at about 0.7 $km^2\ yr^{-1}$ (*26*). This figure is probably an upper bound because some of the regions included in this estimate (such as Beta Regio) may not be centers of significant crustal spreading (*25*) and much of the variation in topographic relief across Aphrodite is not well fit by a simple thermal boundary layer model (*59*). The rate of creation of new lithosphere may be converted to equivalent heat loss if the heat flux attributed to plate spreading is equated to the difference between the heat flow at the surface and that at the base of the plate (*8*) and the lithosphere on Venus more distant than about 2000 km from spreading centers is assumed to have reached thermal steady state (*26*). The contribution of this rate of lithosphere formation to global heat loss (Fig. 2) is then less than about 15% (*26*). A similar figure can be derived as an upper bound on the rate of resurfacing by plate recycling from the density of impact craters on the well-imaged parts of the planet (*53*).

Although sites of horizontal convergence and underthrusting have been identified (*29, 31*), whether these and other sites accommodate 0.7 $km^2\ yr^{-1}$ of lithospheric removal is not known. The four known major mountain belts on Venus, those surrounding Lakshmi Planum in Ishtar Terra, are each about 1000 km in length. Even if these mountain belts were the sites of ongoing convergence at rates of 10 to 40 mm yr^{-1}, the range of half rates obtained from the fit of spreading plate models to topographic profiles across Aphrodite Terra (*59*), then the rate of removal of surface lithosphere at these mountain belts would be only 0.04 to 0.2 $km^2\ yr^{-1}$. Another possibility is that significant lithospheric shortening is occurring across the ridge belts of Venus. The ridge belts in the northern 25% of the Venus surface have a total length of about 4×10^4 km; if the remaining areas have a comparable density of such features, then an average convergence rate in excess of 3 mm yr^{-1} would be required to match the upper bound on rate of lithosphere creation along the equatorial highlands. Whether the total strains accommodated across ridge belts are sufficient to account for such rates of shortening over the time interval spanned by ridge belt deformation is a question which should be addressable with Magellan imaging and gravity data.

It is thus evident that most of the interior heat loss is transported conductively through the Venus lithosphere. This inference permits an estimate of the average thickness of the thermal lithosphere on Venus. For a mantle heat flux of 50 to 70 mW m^{-2}, a temperature at the base of the thermal lithosphere about 100 K hotter than on Earth (*26, 60*), and a lithospheric thermal conductivity of 4 W $m^{-1}\ K^{-1}$ (*61*), the thermal lithosphere on Venus is calculated to be 60 to 80 km thick, one half to two thirds the thickness of the thermal lithosphere in oceanic regions on Earth (*62*).

Most likely the heat flux, lithospheric thermal gradient, and effective lithosphere thickness vary significantly on Venus. Such spatial variations should be strongly linked to patterns of mantle convection. Regions of postulated mantle upwelling, such as broad volcanic rises or coronae, should be areas of enhanced conductive heat flux and thinned lithosphere (*58*) whereas regions of mantle downwelling may be areas of significantly reduced heat flux. Regions of upwelling and downwelling may have diagnostic signatures in long-wavelength topography and gravity (*57, 63*), although variations in crustal thickness and other mechanisms for supporting topographic relief likely complicate simple relations between elevation and heat flow. Evidence should be sought in the Magellan data for such evidence of lateral variations in heat flux as differences in volcanic flux, flexural wavelength variations (*50*), differences in predominant tectonic wavelengths (*64*), or variations in the degree of relaxation of topographic features (*65*).

Crustal formational processes. The formation and evolution of the Venus crust are closely tied to the thermal and dynamical evolution of the interior. Planetary crustal material can be divided into three broad categories (*66*): primary, the result of accretional heating (such as the lunar highland crust); secondary, the result of partial melting of the mantle (such as the lunar maria and the terrestrial oceanic crust); and tertiary, formed by the reprocessing of secondary crustal material (such as terrestrial continental crust). Although Venus may have once had a primary crust, the comparatively young age of the well-imaged parts of the surface (7) and the evidence that sampled surface rocks are basaltic in chemistry and likely to be products of partial melting of the mantle (*41, 67*) support the premise that little or none of any primary crust is present at the Venus surface. Tertiary crustal material requires the remelting of secondary crust, either by basal melting of a thick crustal column or by melting of crustal material recycled by subduction or foundering into the mantle (*68*).

The simplest hypothesis is that most of the crust on Venus is secondary. Under this hypothesis the average thickness and total volume of crust provide a basis for estimating a lower bound on the accumulated volume of magma generated by partial melting of the Venus mantle. Several workers have suggested, largely on theoretical grounds, that the Venus crust may be as thick as 100 km, limited by the depth of the basalt-eclogite transition (*69, 70*). Such a thick crust would have profound effects on interior dynamics. If the surface radioactivity at the Vega 1–2 and Venera 9–10 sites (*41*) is representative of that in the underlying crustal column, then the heat produced in the crust would provide half of the mean heat flux (Fig. 3). Most of such a thick crust would be at high temperature and thus easily deformable and convectively unstable (*47, 70*). Whether such a thick crust with more than half the planetary K content is consistent with the low atmospheric ^{40}Ar abundance (*42, 43*), however, is questionable.

Two lines of evidence suggest that the Venus crust in plains regions at elevations near the planetary mode is typically only 10 to 30 km thick. First, the measured depths of Venus impact craters are permissive of little viscous relaxation of topographic relief over the lifetimes of the craters, a result that requires a layer comparable in strength to the mantle at depths of 10 to 20 km or shallower (*65*). Second, a number of tectonic structures on Venus display two characteristic width or spacing scales, one at 10 to 20 km and one at 100 to 300 km. The most plausible interpretation of this observation is that the two scales are controlled by the thickness of a strong upper crust and the depth to and thickness of a strong upper-mantle layer, and there is quantitative agreement with the observed scales if the crustal thickness in plains regions is generally less

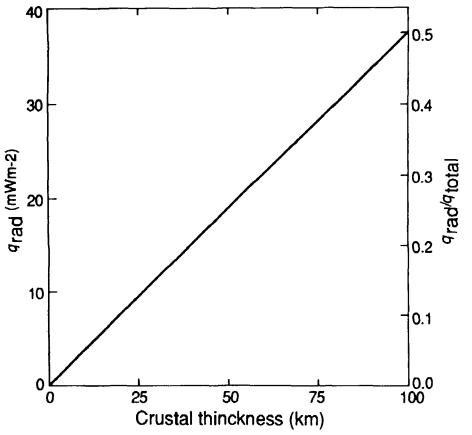

Fig. 3. Contribution of crustal radioactivity to surface heat flow (q_{rad}) as a function of crustal thickness. The crustal abundances of U, Th, and K are taken to be the averages of measured abundances at the Venera 9–10 and Vega 1–2 landing sites (*41*) and are assumed to be uniform with depth. The average surface heat flow q_{total} is taken to be 74 mW m^{-2}, obtained from the assumption that Venus and Earth lose heat at the same rate per planet mass.

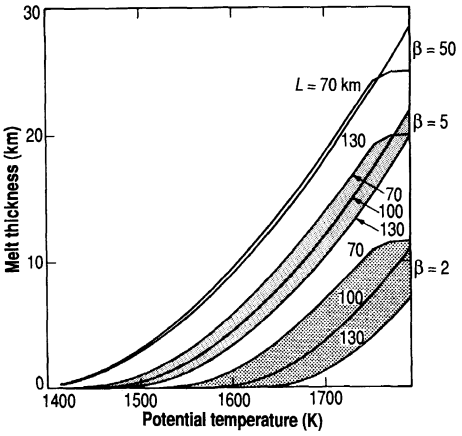

Fig. 4. Thickness of melt layer generated by pressure-release melting of the mantle [after (*74, 75*)]. The potential temperature of the sublithospheric mantle is the temperature it would have if brought to the surface adiabatically without melting. The curves are distinguished by the assumed values of L, the initial thickness of the mechanical boundary layer before lithospheric extension, and the stretching parameter β, given by the ratio of final to initial surface area. The mechanical boundary layer, the outer layer not participating in the convection of the underlying mantle, is somewhat thinner than the thermal lithosphere, for instance, as defined by the plate model for oceanic heat flow and bathymetry on Earth (*62*). A value of L near 70 km is probably appropriate for Venus. The flattening of the curves for L = 70 km at potential temperatures above about 1750 K is because the mantle beneath the mechanical boundary layer is molten even without lithospheric stretching.

than about 30 km (*64, 71*). Correlations of tectonic style with elevation in Ishtar Terra (*30*) suggest that crustal thicknesses in the tessera terrain and mountain belts may exceed that in plains regions by several tens of kilometers. Such thickened crust may provide the only environments in which production of tertiary crust by basal melting or recycling of lower crust by conversion to a dense eclogitic assemblage capable of sinking into the mantle are possible at present on Venus (*68*). Much additional data on both impact crater depths and characteristic tectonic scales will be provided by Magellan.

For an average crustal thickness of 10 to 20 km in plains regions, the global distribution of elevations and simple isostatic considerations indicate that the total crustal volume on Venus is 10^{10} km^3 (*65*). This value is comparable to the present volume of crust on Earth and is about one order of magnitude less than the time-integrated volume of secondary crust produced over all of Earth's history. If little or no crust has been recycled into the mantle on Venus, then average crustal production rates on Venus must be much lower than on Earth. If, on the other hand, crustal production rates have been comparable on the two planets, then some type of crustal recycling must have occurred on Venus in the geologic past (*65, 72*).

These alternatives can be evaluated if an estimate can be made of the rate of addition of new material to the crust. Two routes to such an estimate can be envisioned: (i) determining the volcanic flux and adding a correction to account for magmatic intrusion (*73*), or (ii) estimating melt production from thermal and dynamical models for interior convective flow (*74*). The volcanic flux has not yet been determined directly from observations of the volumes of volcanic units on Venus, but as noted above the density of large impact craters clearly identified on the well-imaged parts of Venus indicate that the average global volcanic flux must have been less than about 2 km^3 yr^{-1} over the past few hundred million years (*53*), a rate equivalent to a mean addition of 4-km crustal thickness per 10^9 years. If the ratio by volume of intrusive to extrusive material is as high as 5 to 10, as it is on Earth (*73*), then this volcanic flux could generate the entire crustal volume on Venus in 10^9 years or less. This flux is only an upper bound, and inclusion of additional circular features of uncertain origin (*52*) in the population of impact craters would lower this bound by an order of magnitude (*54*). Furthermore, the ratio of intrusive to extrusive volumes is a function of the contrasts in both density and temperature between ascending magma and surrounding crustal rock; a dominantly secondary crust on Venus would likely be of greater density and at higher temperature than terrestrial continental crust, which should favor a lesser ratio of intrusive to extrusive material than the highest values on Earth (*73*). Thus the impact crater density is permissive of slow crustal growth and little or no recycling of crust back into the Venus mantle. Direct estimation of rates of volcanism from Magellan images should sharpen this constraint considerably.

Thermal and dynamical convection models that explicitly include melt production and transport have recently been developed for spreading centers and transient plumes (*74–76*). Prediction of melt production rates on Venus from these models, however, requires several assumptions, such as the characteristic temperature and bulk composition of the Venus mantle, the rates of horizontal divergence of the lithosphere over centers of upwelling, and the depth and nature of the boundary layer that is the source for mantle plumes. Parameterized convection calculations of the thermal history of Venus, if all relevant parameters except planet size and surface temperature are assumed to be the same as for Earth and if the atmospheric greenhouse runaway occurred early in Venus history, lead to the prediction that the characteristic temperature of Venus' mantle is about 100 K hotter than Earth's mantle, because the effect of the higher surface temperature at slowing heat loss is greater than the effect of smaller planet size at accelerating interior cooling (*60*). With such a higher characteristic temperature, melt formation at crustal spreading centers would produce a crust about 15 km thick (Fig. 4), or twice as thick as present oceanic crust on Earth (*74, 77*). Even thicker crust could be produced over areas spanning the heads of transient high-temperature plumes (Fig. 4); the volume of melt produced will depend on the excess temperature of the plume and the amount of extension in the overlying lithosphere (*74, 78*). Small changes in one or more parameters in a thermal history calculation, however, can have a large effect on the predicted interior temperature (*60*). As noted above, a reduced lithospheric viscosity on Venus may have led to more efficient heat loss and a Venus mantle now cooler than Earth's mantle (*46*). Furthermore, our ignorance of the relative volatile contents of the mantles of Venus and Earth and of the relation between rheology and the abundances of mantle volatiles is permissive of a wide range of differences in present mantle temperatures on the two bodies (*79*). Of potential significance to this issue are the much greater abundances of nonradiogenic rare gases in the Venus atmosphere than on Earth (*42, 43*); this difference is plausibly attributed to a greater overall inventory of volatiles on Venus than on Earth—including interior water—at the close of planetary accretion (*80*).

Observations from Magellan of the vol-

umes of volcanic materials in various tectonic settings will provide crucial constraints on key parameters of models of interior temperature and volatile content. A global determination of the average age of the surface and estimation of variations in area with age are fundamental to the assessment of the volume of volcanic deposits as a function of time. In addition, the documentation of volcanic styles and their association with tectonic deformation should lead to a better understanding of the ratio of intrusion to extrusion and of the role and volumetric significance of mechanisms of local and regional crustal growth. Finally, a critical assessment of the occurrence of crustal spreading and associated crustal recycling should be possible from Magellan data.

Scales of mantle dynamics. A major challenge in unraveling the evolution of Venus is to understand the interaction between mantle convection and the lithosphere. The strong correlation between long-wavelength gravity and topography and the large (100 to 400 km) apparent depths of compensation of relief for many upland regions (*22*) suggest that these long-wavelength variations are signatures of mantle dynamics (*2, 6*). Furthermore, the large apparent depths of compensation and considerations of probable lithosphere thickness on Venus point to the absence of a low-viscosity zone beneath the lithosphere (*63, 81*), in contrast to the viscosity structure in oceanic regions on Earth (*82*). The lack of a low-viscosity zone, possibly a result of the dehydration of the upper mantle of Venus (*80*), allows mantle dynamic stresses to couple strongly to the overlying lithosphere and can thus contribute significantly to surface topography and tectonic deformation (*81, 83*).

These considerations raise the question as to whether the geometry of upper-mantle convection on Venus may be discerned directly from measurements of topography and gravity and observations of lithospheric deformation and igneous activity. In numerical models of three-dimensional convection in constant-viscosity spherical shells with Rayleigh numbers at about 100 times the critical value, convective upwelling occurs dominantly in the form of cylindrical plumes, and the number and characteristic spacing of plumes are functions of the relative amounts of basal and internal heating (*84*). With parameters appropriate to the Venus mantle and with 20% of the heating supplied from below, a value consistent with the heat flux from the core given by parameterized convection models of Venus thermal evolution (*60*), such calculations indicate that about 20 plumes are active at any one time (*85*), although this result is likely to be quite sensitive to such model assumptions as choice of Rayleigh number and viscosity structure. Localized centers of mantle upwelling are likely to be characterized by broad topographic rises and geoid highs (*86*), uplift and extension of the lithosphere, and consequent pressure-release melting and surface volcanism (*74, 75*). Plumes arising from instability of the bottom boundary layer to upper mantle convection are likely to be transient features on geological time scales (*74, 87*), so that a sequence of events associated with an individual plume on Venus can be anticipated, including initial uplift, voluminous igneous activity, and collapse and relaxation during the waning of plume-delivered heat and magma (*78, 88*). Because of the probable strong coupling of mantle convective stresses to the lithosphere, mantle flow patterns should have predictable associated patterns of surface deformation (*81, 83*). Such diagnostic patterns may be difficult to discern, however, because thin-skinned deformation enabled by a ductile lower crust may in some situations dominate the observable tectonic features (*89*).

Long-wavelength topography and geoid anomalies on Venus are characterized by a number of broad highs such as might be produced by 10 to 20 distinct centers of approximately cylindrical upwelling (*6, 63*), although specification of the geoid is currently limited by the uneven resolution of gravity information with latitude and the necessary truncation of harmonic representations. A number of these highs correspond to broad rises, several thousand kilometers across, that have been identified from radar imaging as centers of volcanism and tectonic activity (*19, 21, 23, 25*), as would be consistent with sites of active mantle upwelling. Many of the details required to associate particular regions on Venus with mantle flow patterns, however, remain to be worked out. For instance, there is not currently agreement as to whether the volcanic plateau Lakshmi Planum in Ishtar Terra (Fig. 1) is located over a region of mantle downwelling, as might be suggested by the large-scale convergence implied by the formation of the bounding mountain belts (*90*), or over a region of mantle upwelling, as might be suggested by the pervasive volcanism (*91*) and aspects of the long-wavelength gravity anomaly (*92*). As discussed above, coronae have also been suggested as sites of mantle upwelling (*16, 17*), although coronae have lesser characteristic dimensions (200 to 1000 km) and are greater in number than the broad highland rises, and coronae do not have a discernible gravity anomaly at present resolution. If both broad rises and coronae are products of mantle upwelling, then multiple scales of mantle convection are indicated, and a physical explanation for the different morphologies of the two classes of features must be found. A complementary problem is the location of sites of mantle downwelling. Theoretical models of mantle convection suggest that downwelling should occur in sheets or cylinders (*84, 85*), and some workers have suggested that much of the downwelling is localized beneath the lowland planitiae (*34, 78*). The lowlands are also sites of pervasive plains volcanism (*11, 33*), however, which would not be expected over regions of convective downwelling and lower than average upper mantle temperatures. Clearly measurements by Magellan of global topography and gravity and delineation of large-scale patterns of volcanism and tectonics and their temporal relations will provide important new information for understanding these issues. It is likely that new models linking magmatism and surface deformation to patterns of interior flow will also be needed.

Two scenarios for global tectonics. On the basis of the above discussion, we offer two simple scenarios for the internal thermal structure of Venus and for the consequent global patterns of volcanism and tectonics:

In the Earth-scaled mantle scenario, the global heat flux and the characteristic mantle temperature have values appropriate to scaling from those quantities on Earth. The average heat flux is about 70 mW m^{-2} (*3*) and the characteristic upper mantle temperature is about 100 K hotter than that on Earth (*26, 60*), or about 1650 to 1700 K (*62, 74*). Volcanism and lithospheric recycling play at most modest roles in lithospheric heat transport (Fig. 2), and heat generation in typical crust 10 to 30 km in thickness (*64, 65, 71*) and with radioactive element abundances appropriate to basaltic material (*40, 41, 67*) contributes only about 10% to the global heat loss (Fig. 3). Thus on average about 50 to 60 mW m^{-2} of mantle heat flux is transported conductively through the Venus lithosphere, and typical thermal gradients are perhaps 10 to 15 K km^{-1} in the lithospheric mantle (*61*) and, because of its lower thermal conductivity (*93*), perhaps 20 to 25 K km^{-1} in the crust. Heat flux and thermal gradients would be expected to display strong regional variations. Because of the comparatively high mantle temperature, significant volumes of melt would be expected to be produced at crustal spreading centers or over mantle plumes at which some lithospheric extension is occurring (Fig. 4). Because of the generally high thermal gradients in the crust, the lower crust should be weak, particularly in elevated regions with crustal thicknesses

greater than the 10 to 20 km typical for plains regions; therefore, thin-skinned tectonics should be evident in such elevated regions (*89*). This scenario thus has two difficulties, although neither is necessarily fatal. A large magmatic flux may be at variance with the surface density of impact craters, as discussed above, although quantification of this statement requires assumptions about the lengths and divergence rates of crustal spreading centers and about the numbers and characteristic temperatures of, and lithospheric extension rates over, major mantle plumes. The support of significant short- to intermediate-wavelength topographic relief and implied thicker crust, most notably in the mountain belts of Ishtar Terra, is made difficult by the high thermal gradients expected for this scenario, even for models in which a dynamic component of support is included. This difficulty might be obviated if such features are in regions of anomalously low heat flow or if the flow laws obtained for crustal materials in terrestrial laboratories are inappropriate to the lower crust of Venus.

In the cool mantle scenario, the characteristic mantle temperature on Venus is less than on Earth (*46*), or less than 1550 to 1600 K (*62, 74*). The average heat flux is also less than in the Earth-scaled mantle scenario, not because heat production is significantly less but rather because secular cooling of the mantle, about 100 K per 10^9 years on Earth (*39*), contributes less to the present heat loss (*46, 47*). The fraction of heat flux contributed by crustal radioactivity is correspondingly larger (Fig. 3), so the mantle heat flux may be 40 mW m^{-2} or less in this scenario. Present magmatism might be quite limited, perhaps restricted to the hot central regions of a few major mantle plumes, so the global volcanic flux should be low. Comparatively low lithospheric thermal gradients would make it easier to support high topographic relief, although some component of dynamic support would probably still be required, particularly for the mountain belts. A lower characteristic mantle temperature might also be accompanied by higher mantle viscosities on Venus than on Earth, a situation that might contribute to the strong correlation of long-wavelength gravity and topography (*2, 6*) and large apparent depths of compensation of long-wavelength relief (*22*). Some elements of this type of scenario for the Venus interior have been discussed by Williams and Pan (*94*). The principal difficulty with this scenario is in providing an explanation for why Venus should have a relatively cool mantle. If both Venus and Earth were comparably heated by the processes of accretion and core-mantle differentiation, then for Venus to have both a lesser characteristic mantle temperature and a lesser rate of cooling at present its interior must have cooled faster than that of Earth; a quantitative explanation for such a more rapid cooling has yet to be developed. Alternatively, if the size of the largest colliding planetesimal during the accretion of Venus was significantly less than that for Earth—a proposed explanation of the much greater abundance of nonradiogenic rare gases on Venus and the absence of a large satellite comparable to Earth's moon (*80*)—Venus may have been left with significantly cooler internal temperatures than Earth at the terminal phase of accretion. Most convective thermal history calculations suggest that the present internal temperature is largely insensitive to characteristic mantle thermal state (*39*), but a modest difference in internal temperatures and cooling rates between the two bodies may nonetheless have persisted.

The two scenarios are potentially distinguishable with data now being provided by the Magellan mission. The Earth-scaled mantle model would be favored by a high global volcanic flux and by indications—from estimates of elastic lithosphere thickness, characteristic tectonic wavelengths, and inferred viscoelastic relaxation times—of high lithospheric thermal gradients. The cool mantle scenario would be favored by evidence for only limited recent volcanism and lesser lithospheric thermal gradients.

Conclusions. At the outset of the Magellan mission it is already clear that Venus shares many tectonic and volcanic characteristics with both Earth and the smaller terrestrial planetary bodies. Structures such as ridge belts and rift zones on Venus are at least qualitatively similar to features observed on Mars, Mercury, and the moon, as well as Earth. Linear mountain belts occur only on Venus and Earth. Venus also displays some structures not seen elsewhere, such as coronae and tessera, although these features are thought to be products of such familiar processes as mantle convection and lithospheric faulting, and analogy with terrestrial landforms may be rendered difficult by the absence of significant weathering and erosion on Venus. Volcanism on Venus is often associated with regions of apparent mantle upwelling, as on Earth, but volcanic plains are widespread as on the smaller terrestrial planets, and the link between plains volcanism and mantle dynamics is not understood. Crustal spreading and recycling may have occurred on Venus in the past or may even be occurring at limited rates at present, but the dominant mechanism of lithospheric heat loss on Venus appears to be conduction as on the smaller terrestrial planets. Determination of the global distribution of specific types of features, their ages, and their modes of origin is required, however, before a comprehensive view of the geological evolution of Venus can be made. Estimates of volcanic flux, lithospheric thermal gradients, lithospheric strain rates, and their regional variations as well as improved measurements of global topography and gravity are needed to test and to sharpen hypotheses on the interior heat budget and thermal structure, the mechanical structure of the lithosphere, and the characteristics of mantle convection. Data from Magellan should significantly advance our understanding in all of these areas.

REFERENCES AND NOTES

1. The lithosphere is the outer 100 km or so of a planet or satellite displaying long-term mechanical strength.
2. R. J. Phillips, W. M. Kaula, G. E. McGill, M. C. Malin, *Science* **212**, 879 (1981).
3. S. C. Solomon and J. W. Head, *J. Geophys. Res.* **87**, 9236 (1982).
4. G. H. Pettengill *et al.*, *ibid.* **85**, 8261 (1980).
5. H. Masursky *et al.*, *ibid.*, p. 8232.
6. B. G. Bills, W. S. Kiefer, R. L. Jones, *ibid.* **92**, 10,335 (1987).
7. B. A. Ivanov, A. T. Basilevsky, V. P. Kryuchkov, I. M. Chernaya, *Proc. 16th Lunar Planet. Sci. Conf., J. Geophys. Res.* **91**, D413 (1986); G. G. Schaber, E. M. Shoemaker, R. C. Kozak, *Sol. Syst. Res.* **21**, 89 (1987); D. B. Campbell, N. J. S. Stacy, A. A. Hine, *Geophys. Res. Lett.* **17**, 1389 (1990).
8. J. G. Sclater, C. Jaupart, D. Galson, *Rev. Geophys. Space Phys.* **18**, 269 (1980).
9. R. Greeley and R. E. Arvidson, *Earth Moon Planets* **50/51**, 137 (1990).
10. G. H. Pettengill, P. G. Ford, B. D. Chapman, *J. Geophys. Res.* **93**, 14,881 (1988); D. L. Bindschadler and J. W. Head, *Earth Moon Planets* **42**, 133 (1988).
11. A. L. Sukhanov *et al.*, *U. S. Geol. Survey Misc. Invest. Ser.* Map I-2059 (1989).
12. J. C. Aubele and E. N. Slyuta, *Earth Moon Planets* **50/51**, 493 (1990).
13. E. N. Slyuta and M. A. Kreslavsky, *Lunar Planet. Sci.* **21**, 1174 (1990).
14. E. N. Slyuta, *ibid.*, p. 1172; G. G. Schaber, *Proc. Lunar Planet. Sci.* **21**, 3 (1991).
15. V. L. Barsukov *et al.*, *Proc. 16th Lunar Planet. Sci. Conf., J. Geophys. Res.* **91**, D378 (1986).
16. A. T. Basilevsky *et al.*, *ibid.*, p. D399.
17. A. A. Pronin and E. R. Stofan, *Icarus* **87**, 452 (1990).
18. E. R. Stofan and J. W. Head, *ibid.* **83**, 216 (1990).
19. D. B. Campbell *et al.*, *Science* **246**, 373 (1989).
20. E. R. Stofan and R. S. Saunders, *Geophys. Res. Lett.* **17**, 1377 (1990).
21. D. A. Senske, *Earth Moon Planets* **50/51**, 305 (1990).
22. S. E. Smrekar and R. J. Phillips, *Earth Planet. Sci. Lett.*, in press.
23. D. B. Campbell, J. W. Head, J. K. Harmon, A. A. Hine, *Science* **226**, 167 (1984).
24. G. G. Schaber, *Geophys. Res. Lett.* **9**, 499 (1982).
25. G. E. McGill, S. J. Steenstrup, C. Barton, P. G. Ford, *ibid.* **8**, 737 (1981).
26. W. M. Kaula and R. J. Phillips, *ibid.*, p. 1187.
27. J. W. Head III and L. S. Crumpler, *Science* **238**, 1380 (1987); *Nature* **346**, 525 (1990).
28. L. S. Crumpler, J. W. Head III, J. K. Harmon, *Geophys. Res. Lett.* **14**, 607 (1987); L. S. Crumpler and J. W. Head, *J. Geophys. Res.* **93**, 301 (1988).
29. L. S. Crumpler, J. W. Head, D. B. Campbell, *Geology* **14**, 1031 (1986).
30. R. W. Vorder Bruegge and J. W. Head, *Geophys. Res. Lett.* **16**, 699 (1989).
31. J. W. Head, *Geology* **18**, 99 (1990).
32. S. L. Frank and J. W. Head, *Earth Moon Planets* **50/51**, 421 (1990).

33. D. B. Campbell, D. A. Senske, J. W. Head, A. A. Hine, P. C. Fisher, *Science* **251**, 180 (1991).
34. M. T. Zuber, *Geophys. Res. Lett.* **17**, 1369 (1990).
35. V. P. Kryuchkov, *Lunar Planet. Sci.* **19**, 649 (1988).
36. A. L. Sukhanov and A. A. Pronin, *Proc. 19th Lunar Planet. Sci. Conf.* (1989), p. 335.
37. J. W. Head, *J. Geophys. Res.* **95**, 7119 (1990).
38. D. L. Bindschadler and J. W. Head, *J. Geophys. Res.*, in press.
39. BVSP (Basaltic Volcanism Study Project), *Basaltic Volcanism on the Terrestrial Planets* (Pergamon, New York, 1981).
40. Yu. A. Surkov, *Proc. 8th Lunar Sci. Conf.* (1977), p. 2665.
41. Yu. A. Surkov *et al.*, *Proc. 17th Lunar Planet. Sci. Conf., J. Geophys. Res.* **92**, E537 (1987).
42. J. H. Hoffman, R. R. Hodges, T. M. Donahue, M. B. McElroy, *J. Geophys. Res.* **85**, 7882 (1980).
43. T. M. Donahue and J. B. Pollack, in *Venus*, D. M. Hunten, L. Colin, T. M. Donahue, V. I. Moroz, Eds. (Univ. of Arizona Press, Tucson, 1983), pp. 1003–1036.
44. D. L. Turcotte and K. Burke, *Earth Planet. Sci. Lett.* **41**, 341 (1978).
45. D. McKenzie and F. M. Richter, *J. Geophys. Res.* **86**, 11,667 (1981).
46. J. Arkani-Hamed and M. N. Toksöz, *Phys. Earth Planet. Inter.* **34**, 232 (1984); N. H. Sleep, M. A. Richards, B. H. Hager, *J. Geophys. Res.* **93**, 7672 (1988).
47. V. S. Solomatov and V. N. Zharkov, *Icarus* **84**, 280 (1990).
48. M. K. McNutt, *J. Geophys. Res.* **89**, 11,180 (1984).
49. S. C. Solomon and J. W. Head, *Lunar Planet. Sci.* **21**, 1180 (1990).
50. ———, *Geophys. Res. Lett.* **17**, 1393 (1990).
51. D. L. Turcotte, *J. Geophys. Res.* **94**, 2779 (1989).
52. A. T. Basilevsky *et al.*, *ibid.* **92**, 12,869 (1987).
53. R. E. Grimm and S. C. Solomon, *Geophys. Res. Lett.* **14**, 538 (1987).
54. R. E. Arvidson, R. E. Grimm, R. J. Phillips, G. G. Schaber, E. M. Shoemaker, *ibid.* **17**, 1385 (1990).
55. B. Fegley, Jr., and R. G. Prinn, *Nature* **337**, 55 (1989).
56. J. A. Wood and A. Hashimoto, *Lunar Planet. Sci.* **22**, 1519 (1991).
57. R. J. Phillips and M. C. Malin, in *Venus*, D. M. Hunten, L. Colin, T. M. Donahue, V. I. Moroz, Eds. (Univ. of Arizona Press, Tucson, 1983), pp. 159–214.
58. P. Morgan and R. J. Phillips, *J. Geophys. Res.* **88**, 8305 (1983).
59. R. E. Grimm and S. C. Solomon, *ibid.* **94**, 12,103 (1989).
60. D. J. Stevenson, T. Spohn, G. Schubert, *Icarus* **54**, 466 (1983).
61. J. F. Schatz and G. Simmons, *J. Geophys. Res.* **77**, 6966 (1972).
62. B. Parsons and J. G. Sclater, *ibid.* **82**, 803 (1977).
63. W. S. Kiefer, M. A. Richards, B. H. Hager, B. G. Bills, *Geophys. Res. Lett.* **13**, 14 (1986).
64. M. T. Zuber, *Proc. 17th Lunar Planet. Sci. Conf., J. Geophys. Res.* **92**, E541 (1987); M. T. Zuber and E. M. Parmentier, *Icarus* **85**, 290 (1990).
65. R. E. Grimm and S. C. Solomon, *J. Geophys. Res.* **93**, 11,911 (1988).
66. S. R. Taylor, *Tectonophysics* **161**, 147 (1989).
67. Yu. A. Surkov, V. L. Barsukov, L. P. Moskalyeva, V. P. Kharyukova, A. L. Kemurdzhian, *Proc. 14th Lunar Planet. Sci. Conf., J. Geophys. Res.* **89**, B393 (1984).
68. P. C. Hess and J. W. Head, *Earth Moon Planets* **50/51**, 57 (1990).
69. D. L. Anderson, *Geophys. Res. Lett.* **7**, 101 (1980).
70. W. M. Kaula, *Lunar Planet. Sci.* **19**, 593 (1988).
71. W. B. Banerdt and M. P. Golombek, *J. Geophys. Res.* **93**, 4759 (1988).
72. J. W. Head, *Earth Moon Planets* **50/51**, 5 (1990).
73. J. A. Crisp, *J. Volcanol. Geotherm. Res.* **20**, 177 (1984).
74. R. White and D. McKenzie, *J. Geophys. Res.* **94**, 7685 (1989).
75. D. McKenzie and M. J. Bickle, *J. Petrol.* **29**, 625 (1988).
76. D. R. Scott and D. J. Stevenson, *J. Geophys. Res.* **94**, 2973 (1989).
77. C. Sotin, D. A. Senske, J. W. Head, E. M. Parmentier, *Earth Planet. Sci. Lett.* **95**, 321 (1989).
78. R. J. Phillips, R. E. Grimm, M. C. Malin, *Science* **252**, 288 (1991).
79. P. J. McGovern and S. C. Solomon, *Lunar Planet. Sci.* **20**, 669 (1989).
80. W. M. Kaula, *Science* **247**, 1191 (1990).
81. R. J. Phillips, *J. Geophys. Res.* **95**, 1301 (1990).
82. E. M. Robinson, B. Parsons, S. F. Daly, *Earth Planet. Sci. Lett.* **82**, 335 (1987).
83. R. J. Phillips, *Geophys. Res. Lett.* **13**, 1141 (1986).
84. D. Bercovici, G. Schubert, G. A. Glatzmaier, *Science* **244**, 950 (1989).
85. G. Schubert, D. Bercovici, G. A. Glatzmaier, *J. Geophys. Res.* **95**, 14,105 (1990).
86. B. Parsons and S. Daly, *ibid.* **88**, 1129 (1983).
87. M. A. Richards, R. A. Duncan, V. E. Courtillot, *Science* **246**, 103 (1989).
88. R. R. Herrick and R. J. Phillips, *Geophys. Res. Lett.* 17, 2129 (1990).
89. S. E. Smrekar and R. J. Phillips, *ibid.* **15**, 693 (1988).
90. W. S. Kiefer and B. H. Hager, *Lunar Planet. Sci.* **20**, 520 (1989); D. L. Bindschadler, G. Schubert, W. M. Kaula, *Geophys. Res. Lett.* **17**, 1345 (1990).
91. A. A. Pronin, *Geotectonics* **20**, 271 (1986); A. T. Basilevsky, *ibid.*, p. 282.
92. R. E. Grimm and R. J. Phillips, *Geophys. Res. Lett.* **17**, 1349 (1990).
93. S. P. Clark, Jr., in *Handbook of Physical Constants, Memoir 97*, S. P. Clark, Ed. (Geological Society of America, Boulder, CO, 1966) pp. 459–482.
94. D. R. Williams and V. Pan, *Geophys. Res. Lett.* **17**, 1397 (1990).
95. We thank D. McKenzie for performing the calculations depicted in Fig. 4, and W. M. Kaula, G. G. Schaber, and N. H. Sleep for helpful comments on an earlier draft. S.C.S. was a Visiting Associate in the Division of Geological and Planetary Sciences, California Institute of Technology, during the writing of this manuscript. This research was supported by the National Aeronautics and Space Administration under contracts 957070 and 957088 from the Jet Propulsion Laboratory and grants NAGW-1937 and NAGW-713.

8 January 1991; accepted 25 February 1991

Magellan: Radar Performance and Data Products

GORDON H. PETTENGILL, PETER G. FORD, WILLIAM T. K. JOHNSON, R. KEITH RANEY, LAURENCE A. SODERBLOM

The Magellan Venus orbiter carries only one scientific instrument: a 12.6-centimeter-wavelength radar system shared among three data-taking modes. The synthetic-aperture mode images radar echoes from the Venus surface at a resolution of between 120 and 300 meters, depending on spacecraft altitude. In the altimetric mode, relative height measurement accuracies may approach 5 meters, depending on the terrain's roughness, although orbital uncertainties place a floor of about 50 meters on the absolute uncertainty. In areas of extremely rough topography, accuracy is limited by the inherent line-of-sight radar resolution of about 88 meters. The maximum elevation observed to date, corresponding to a planetary radius of 6062 kilometers, lies within Maxwell Mons. When used as a thermal emission radiometer, the system can determine surface emissivities to an absolute accuracy of about 0.02. Mosaicked and archival digital data products will be released in compact disk (CDROM) format.

MAGELLAN'S RADIO AND RADAR observations of Venus involve three distinct modes of operation: (i) side-looking synthetic aperture (SAR) imaging, (ii) nadir-directed altimetry, and (iii) thermal emission radiometry. The observations are carried out with a common radar instrument comprising eight units that are completely duplicated onboard to provide double-string operational redundancy. (As of the end of December 1990, there have been no failures in the radar, and all units are still drawn only from the prime system.) The performance of the radar in each of these time-shared modes is detailed in separate sections below.

The design of the Magellan radar system reflects the mission's scientific objectives, which include the imaging of more than 70% of the surface of Venus at a resolution of better than 360 m and a determination of a corresponding part of the planet's topography with a height resolution commensurate with the imaging waveform. The radar system as implemented can image about 90% of the surface during the first 8 months of the mission, and more than half of that is at a resolution of better than 130 m. It should eventually be able to map the entire planetary surface, using data obtained in additional mapping cycles extending beyond the first 8 months of operation.

The transmitter, receiver, waveform generator, and timing systems (Table 1) are shared among the three operating modes. In the two radar modes, the transmitter employs a pulse consisting of 60 elements of a biphase code that has been carefully chosen to minimize time-delay sidelobes. By the use of an amplitude-tapered decoding (compression) sequence, the point-spread func-

G. H. Pettengill and P. G. Ford, Massachusetts Institute of Technology, Cambridge, MA 02139.
W. T. K. Johnson, Jet Propulsion Laboratory, California Institute of Technology, Pasadena, CA 91109.
R. Keith Raney, Canada Centre for Remote Sensing, Ottawa, Ontario K1A 0Y7, Canada.
L. A. Soderblom, U.S. Geological Survey, Flagstaff, AZ 86001.